On the Impact of Carrier Phase Estimation on Phase Correlations in Coherent Fiber Transmission

Tobias Fehenberger* and Norbert Hanik
Institute for Communications Engineering
Technische Universität München
80333 Munich, Germany
*Email: tobias.fehenberger@tum.de

Tobias A. Eriksson, Pontus Johannisson,
and Magnus Karlsson
Department of Microtechnology and Nanoscience
Chalmers University of Technology
SE-41296 Gothenburg, Sweden

***Abstract*—Carrier phase estimation (CPE) is an integral part of the digital signal processing (DSP) of coherent optical communication systems as it compensates laser phase noise (LPN) introduced by free-running transmitter and local oscillating (LO) lasers. Nonlinear interactions during propagation are another source of correlated phase noise. In this paper, we show through simulations and in experiments that blind decision-directed (DD) CPE with regular block lengths removes a large portion of the memory. This makes it virtually impossible in practice to quantify correlations that come from propagation effects, or to obtain rate gains by exploiting the nonlinear phase noise (NLPN). Larger CPE block lengths leave the memory partly intact. This, however, comes at the expense of reduced information rates. We are able to fully recover this rate loss in simulations by using idealized processing of phase distortions. In experiments with full DSP, an almost full rate recovery is reported.**

I. Introduction

Lower bounds on the capacity of optical fiber links have attracted a lot of attention in recent years, mostly because they can serve as a benchmark to achievable information rates (AIRs) and spectral efficiencies of experiments and commercial systems. Recently, well-known lower bounds [1] have been improved [2]–[4] by exploiting correlations in the phase that originate from fiber nonlinearities [5]. This nonlinear phase noise (NLPN) can be modeled as a Wiener process [4] and partly compensated by exploiting the underlying correlations.

In coherent optical fiber systems, a free-running laser is used at the transmitter and as local oscillator (LO) in the receiver. Because the linewidth of practical lasers is typically in the range of several tens of kHz up to a few MHz [6], carrier phase estimation (CPE) is required to compensate the phase distortions. This carrier phase recovery is usually part of the digital signal processing (DSP) [7]. Both laser phase noise (LPN) and NLPN are present simultaneously. In this paper, we study through simulations and in experiments how LPN with subsequent phase noise compensation affects the AIRs and the memory in the received symbols. The auto-correlation function (ACF) allows to quantify the residual memory after propagation and DSP. If correlations are found, they could be exploited by a subsequent algorithm to achieve improved information rates. To the best of our knowledge, this work is the first experimental analysis of memory and achievable rates when phase distortions from lasers and fiber propagation are present and compensated.

II. Compensation of Phase Distortions

A. Carrier Phase Estimation (CPE)

LPN is often modeled as a Wiener noise process [8], [9], which is a random walk of Gaussian variables with zero mean and variance that is proportional to the combined linewidth of the transmitter and the LO laser. Different algorithms have been presented to compensate this deterministic distortion, such as the Viterbi-Viterbi algorithm [10]. To improve this method for quadrature amplitude modulation (QAM), partitioning schemes have been introduced, e.g. in [11]. A decision-directed (DD) approach that uses test phases and is valid for any QAM has been proposed in [6]. We use this algorithm to compensate LPN and outline its principle briefly in the following. We generate B test phases that are uniformly distributed over $[0, \frac{\pi}{2}[$. The received symbols y_k are rotated by these phases, resulting in B rotated versions of the channel output. For every rotated symbol, the squared Euclidean distance to its closest constellation point is calculated. Next, the sum over $2N+1$ distance values is computed to average out uncorrelated complex Gaussian noise. In the last step, the test phase that gives the minimum sum is chosen for rotating back the symbol in the center of the block. This is repeated for every received symbol. We choose 32 test phases throughout this work.

B. Phase Noise (PN) Receiver

A phase noise (PN) receiver has been proposed in [4] to show AIR gains by exploiting the correlated NLPN. The PN receiver is an idealized algorithm that assumes perfect knowledge of past sent symbols x, and thus serves as a reference for blind phase tracking algorithms. Placed as the last stage of the DSP, the PN receiver computes the mean angle $\bar{\phi}_k$ of w past symbols,

$$\bar{\phi}_k = \measuredangle \sum_{l=1}^{w} x_{k-l}^* \cdot y_{k-l}, \tag{1}$$

where x_k^* is the complex conjugate of the symbol x_k that is sent at time instance k, and y_k is the corresponding received

symbol after DSP. The phase distortion of y_k is then undone by a phase rotation,

$$y'_k = y_k \cdot \exp(-j\bar{\phi}_k). \tag{2}$$

The AIR of the PN receiver is calculated with y'_k instead of y_k.

III. Simulation and Experimental Setup

Simulations with idealized parameters are carried out to isolate the impact that CPE and the PN receiver have on the ACFs and AIRs. A sequence of 250,000 16-QAM symbols is created at a symbol rate of 20 GBaud, digitally pulse-shaped with a root-raised cosine (RRC) filter with 50% roll-off, and modulated onto a carrier at 1550 nm. The laser linewidth is either zero when no LPN is considered, or 200 kHz (counting for both transmitter and LO laser) when LPN is investigated. The dual-polarization optical signal consists of 7 wavelength-division multiplexing (WDM) channels spaced at 30 GHz. The optical launch power is 3 dBm per WDM channel. This power level is several dB above the optimum power such that we operate in a regime where strong nonlinear effects occur. This potentially allows for easier characterization of the NLPN as its variance grows with signal power.

The fiber link consists of a standard single-mode fiber with 0.2 dB/km attenuation, 17 ps/nm/km dispersion, and a nonlinear coefficient of 1.3 1/W/km. Polarization mode dispersion (PMD) is neglected in the simulations. The signal is propagated over 14 spans of 80 km length (total length 1120 km). Every span is followed by an EDFA with 4 dB noise figure. The signal propagation in the fiber is simulated using the split step Fourier method with 32 samples per symbol and a step size of 0.1 km.

At the receiver, the center WDM channel is extracted with an ideal band-pass filter, and chromatic dispersion is compensated. A RRC filter is used as matched filter. When CPE is performed, we use CPE algorithm presented in Section II-A. If the symbols are to be processed further, the PN receiver of Section II-B is used. Finally, AIRs are calculated assuming Gaussian noise statistics [12]. In order to quantify the correlations in the phase of y_k, the ACF of the averaged phase is determined, which is based on the block-wise constant phase model [2]. The averaging is required to cancel out uncorrelated additive Gaussian noise terms that would otherwise dominate over the correlated phase noise due to their larger variance, which would result in an ACF that resembles a Dirac delta function. The phase difference of a received symbol to its corresponding sent symbol is $\measuredangle(x_k^* \cdot y_k)$. The moving average over a block of length w' is

$$\bar{\theta}_k = \measuredangle \sum_{m=-\frac{w'-1}{2}}^{\frac{w'-1}{2}} x^*_{k-m} \cdot y_{k-m}, \tag{3}$$

Note that in contrast to Eq. (1), the average $\bar{\theta}_k$ is determined in the center of a window and thus includes future and past symbols. The ACF is then computed with $\bar{\theta}_k$.

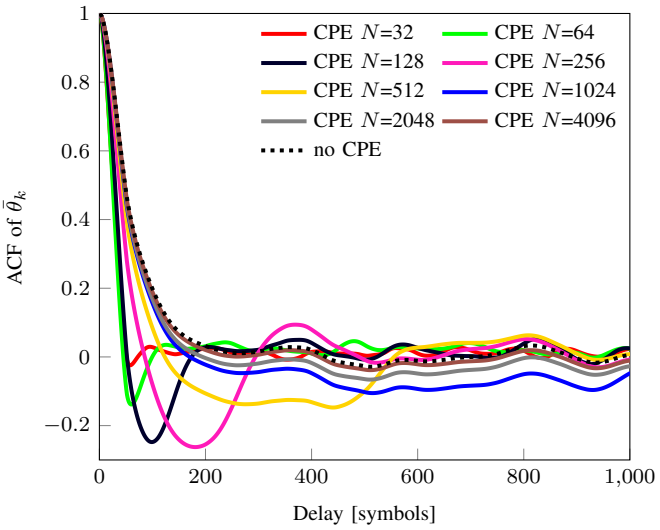

Fig. 1. ACF for simulations without LPN and for different CPE lengths N. All ACFs are obtained with $w' = 51$.

TABLE I
AIRs for simulations without LPN

CPE N	AIR [bit/sym]	AIR w/ PN receiver ($w = 6$)
32	3.51	3.57
64	3.65	3.71
128	3.70	3.77
256	3.70	3.80
512	3.70	3.82
1024	3.70	3.82
2048	3.70	3.82
4096	3.69	3.82
No CPE	3.69	3.82

The parameters of the experiment are chosen to match the simulations as closely as feasible. The fiber link is a recirculating loop with a polarization scrambler after every round-trip, with a total length of 1120 km. The transmitter laser and the LO laser have a linewidth of approximately 100 kHz each. In the receiver, we use a full DSP structure with polarization-demultiplexing and adaptive equalization based on DD least-mean square [11] and the DD CPE outlined in Section II-A for phase estimation.

IV. Results

A. Simulations without LPN

The ACFs for simulations without LPN are depicted in Fig. 1. In this case, the only source of correlated phase noise is NLPN. CPE is not required in the DSP, yet illustrates how the NLPN is affected by CPE. The ACF without CPE (dotted) is the reference curve showing how much correlations from nonlinear propagation effects are present. When CPE is performed, the shape of the ACF varies significantly with the block length N. A small N reduces the ACF length, i.e., it removes memory, as the CPE does not capture the phase correlations that are spread over many symbols but has its decision strongly influenced by additive white Gaussian noise. For increasing N, the ACF with CPE approaches the ACF

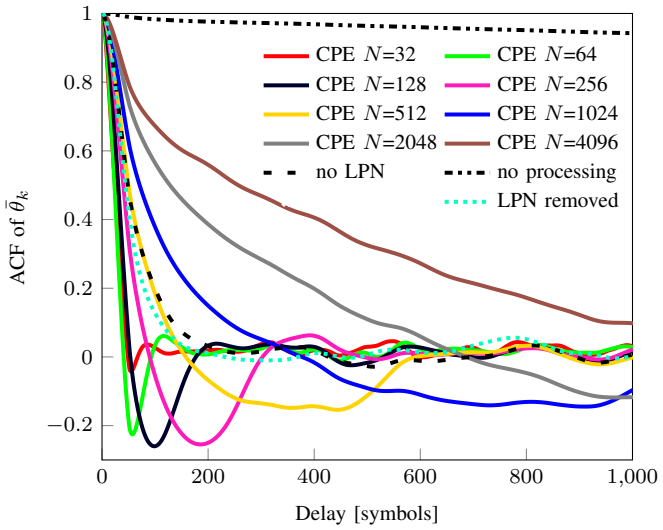

Fig. 2. ACF for simulations with LPN (laser linewidth 200 kHz) and for different CPE lengths N. All ACFs are obtained with $w' = 51$.

TABLE II
AIRs FOR SIMULATIONS WITH LPN

CPE N	AIR [bit/sym]	AIR w/ PN receiver ($w = 6$)
32	3.73	3.73
64	3.73	3.77
128	3.70	3.70
256	3.68	3.80
512	3.64	3.81
1024	3.59	3.81
2048	3.48	3.81
4096	3.24	3.81
Removed LPN	3.69	3.82
No CPE	0.01	3.82

without CPE for delays of up to 300 symbols. The reason behind this is that for a large N, the CPE is performed over many symbols that are only weakly correlated, or not correlated at all. Taking the average over this large block gives a phase estimate of approximately 0 radians, and the CPE does not perform any rotation.

The AIRs that correspond to the ACFs of Fig. 1 are given in Table I. The reference AIR of 3.69 bits per symbol (bit/sym) is obtained without any phase processing, and 3.82 bit/sym is achievable if the PN receiver is employed. Throughout this work, the length w of the PN receiver is chosen heuristically such that the largest AIR is observed. For small block lengths of $N = 32$ or $N = 64$, the AIRs with CPE are smaller than the no-processing reference, which follows the same argument as for the ACF. With CPE block lengths of $N = 128$ and larger, the AIRs saturate close to the reference.

If PN processing is employed, the AIR can be increased to 3.82 bit/sym by exploiting the NLPN correlations. This gain of 0.13 bit/sym is in the order to what other studies [3] have reported over a link with lumped amplification. We observe that smaller AIRs are obtained when CPE is employed, which motivates the use of more sophisticated phase tracking algorithms.

B. Simulations with LPN

ACFs and AIRs for a total laser linewidth of 200 kHz are shown in Fig. 2 and Table II, respectively. When LPN is present yet uncompensated, the ACF shows strong correlations in the phase of the received symbols. With CPE, the ACF is reduced as CPE removes some of the correlations. When the block length is chosen very large, the ACF approaches the curve without processing. The explanation for this follows the same argument as before: CPE becomes ineffective for large N and much of the phase correlation of the LPN remains unused. Further simulations confirm this to also be true when fiber nonlinearities are not present.

Without the PN receiver, a reference AIR of 3.69 bit/sym is obtained by ideal cancellation of LPN. This is done by storing the actual LPN realizations and removing the phase distortions ideally in the DSP. This approach is impossible in practice yet interesting to consider as it gives the AIR when LPN is removed ideally, yet without using NLPN correlations. We also observe from this analysis that the AIR for ideally removed CPE equals the AIR for simulations without LPN and CPE (last row of Table I). The conclusion is that, within the limits of this analysis, LPN has no impact on the propagation effects. When LPN is not compensated, the AIR is approximately 0 bit/sym. For N between 32 and 128, the reference AIR of 3.69 bit/sym is exceeded. Hence, CPE is able to exploit correlations that are not from the lasers but from nonlinear propagation effects. This is expected because LPN and NLPN can be considered a joint Wiener process. For a CPE length N of 256, the AIR is approximately equal to the reference of 3.69 bit/sym. Larger block lengths result in a decrease in rate because LPN is canceled less effectively, for the same reasons as in the simulations without LPN. If we include the PN receiver, the AIR is increased for large N and almost reaches the maximum of 3.82 bit/sym. CPE with small N exploits some of the phase correlations, but the reduced memory (see the ACF in Fig. 2) render it impossible for the PN receiver to reach the maximum of 3.82 bit/sym.

C. Experiments

The ACF for the experimentally obtained QAM symbols is depicted in Fig. 3. We observe that a small CPE length N leaves only a small amount of correlation, while for large N, a large portion of the memory is still present. Since CPE is an integral part of the DSP, measuring correlations in the NLPN using the ACF becomes virtually impossible for reasonable choices of N. For all considered block lengths, the ACF features peaks that occur at the same position, such as at a delay of 70 symbols and close to 200 symbols. The origin and the position of these peaks are not entirely clear. Table III shows a maximum AIR of 3.49 bit/sym for CPE with $N = 128$. The difference of 0.2 bit/sym in comparison to the maximum AIR of the simulations reflects the implementation penalty of the experiment. With increasing N, the experimental AIR decreases because the CPE window becomes too large, which degrades the phase tracking performance. If the PN receiver is employed, the AIR remains approximately equal to the AIR

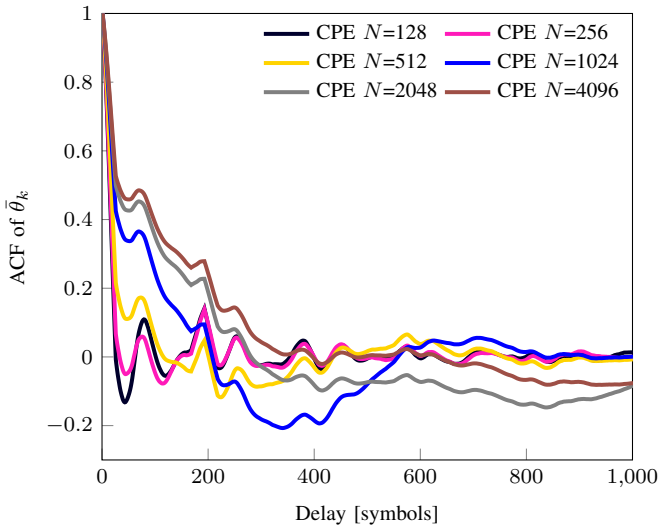

Fig. 3. ACF (experimental) for different CPE lengths N. All ACFs are obtained with $w' = 25$.

TABLE III
EXPERIMENTAL AIRS

CPE N	AIR [bit/sym]	AIR w/ PN receiver
128	3.49	3.48 ($w = 210$)
256	3.48	3.47 ($w = 270$)
512	3.44	3.43 ($w = 90$)
1024	3.34	3.43 ($w = 90$)
2048	3.29	3.43 ($w = 90$)
4096	3.26	3.43 ($w = 90$)

without PN processing for N up to 512. For larger block lengths, the CPE does not cancel all LPN, and the PN receiver is able to recover the rate loss.

V. CONCLUSION

We investigate in simulations and experiments the impact of CPE on the ACF and the AIRs of optical fiber systems. Experimental results show that CPE alters the phase correlations significantly. For normal block lengths, virtually no correlations in the phase are present after CPE, and NLPN cannot be tracked. The fact that rate gains are not feasible with the idealized PN receiver supports this finding. In order to enable higher information rates, the correlations introduced by nonlinear propagation effects must be exploited. Advanced CPE algorithms play a major role in this as they operate on the joint Wiener process of LPN and NLPN. Other methods than the presented ACF calculation in the DSP must be thought of if the memory is to be characterized. A different approach is to use self-homodyne detection [13], which requires no phase tracking at all.

REFERENCES

[1] R.-J. Essiambre, G. Kramer, P. J. Winzer, G. J. Foschini, and B. Goebel, "Capacity limits of optical fiber networks," *J. Lightw. Technol.*, vol. 28, no. 4, pp. 662–701, Feb. 2010.

[2] R. Dar, M. Feder, A. Mecozzi, and M. Shtaif, "Properties of nonlinear noise in long, dispersion-uncompensated fiber links," *Optics Express*, vol. 21, no. 22, pp. 25 685–99, Nov. 2013.

[3] M. Secondini and E. Forestieri, "On XPM mitigation in WDM fiber-optic systems," *IEEE Photon. Technol. Lett.*, vol. 26, no. 22, pp. 2252–2255, Nov. 2014.

[4] T. Fehenberger, M. P. Yankov, L. Barletta, and N. Hanik, "Compensation of XPM interference by blind tracking of the nonlinear phase in WDM systems with QAM input," in *European Conference on Optical Communication (ECOC)*, accepted for publication, 2015.

[5] A. Mecozzi and R.-J. Essiambre, "Nonlinear Shannon limit in pseudolinear coherent systems," *J. Lightw. Technol.*, vol. 30, no. 12, pp. 2011–2024, Jun. 2012.

[6] T. Pfau, S. Hoffmann, and R. Noé, "Hardware-efficient coherent digital receiver concept with feedforward carrier recovery for m-QAM constellations," *J. Lightw. Technol.*, vol. 27, no. 8, pp. 989–999, Apr. 2009.

[7] S. J. Savory, "Digital coherent optical receivers: algorithms and subsystems," *IEEE J. Sel. Topics Quantum Electron.*, vol. 16, no. 5, pp. 1164–1179, Sep. 2010.

[8] F. Munier, E. Alpman, T. Eriksson, A. Svensson, and H. Zirath, "Estimation of phase noise for QPSK modulation over AWGN channels," in *Proc. GigaHertz 2003 Symp*, Linköping, Sweden, Nov. 2003.

[9] E. Ip and J. M. Kahn, "Feedforward carrier recovery for coherent optical communications," *J. Lightw. Technol.*, vol. 25, no. 9, pp. 2675–2692, Sep. 2007.

[10] A. J. Viterbi and A. M. Viterbi, "Nonlinear estimation of PSK-modulated carrier phase with application to burst digital transmission," *IEEE Trans. Inf. Theory*, vol. 29, no. 4, pp. 543–551, Jul. 1983.

[11] I. Fatadin, D. Ives, and S. J. Savory, "Blind equalization and carrier phase recovery in a 16-QAM optical coherent system," *J. Lightw. Technol.*, vol. 27, no. 15, pp. 3042–3049, Aug 2009.

[12] T. Fehenberger, A. Alvarado, P. Bayvel, and N. Hanik, "On achievable rates for long-haul fiber-optic communications," *Optics Express*, vol. 23, no. 7, pp. 9183 – 9191, Apr. 2015.

[13] T. Miyazaki and F. Kubota, "PSK self-homodyne detection using a pilot carrier for multibit/symbol transmission with inverse-RZ signal," *IEEE Photon. Technol. Lett.*, vol. 17, no. 6, pp. 1334–1336, Jun. 2005.